STUDY OF THE DISCHARGE PROCESS INTO A LIQUID OF A GAS STREAM FROM AN IMMERSED NOZZLE

I. P. Ginzburg, V. A. Surin,
A. A. Bagautdinov, A. S. Grigor'yants,
and L. I. Shub

UDC 532.529.5

The results of an experimental investigation of the discharge into a liquid of a gas stream from an immersed nozzle, positioned at an arbitrary angle to the surface, are presented. It is assumed that the gas is not dissolved in the liquid, i.e., it is nonassimilable.

Investigational Procedure

The investigations were carried out on transparent models, the layouts and basic parameters of which are presented in Fig. 1 and in Table 1. In carrying out the experiments, the instantaneous values of the pressure in the prenozzle space and also the parameters of the gas flow, averaged with time, were determined: the feed pressure P_0, the gas flow rate G, and the total and static (P_a) pressures at the nozzle scarf; flow visualization of the jet and of the secondary gas formations in plane and axisymmetrical models was effected with recordings of the hydrogasdynamic process by moving-picture and frame photography methods. The framing speed was 3000 frames/sec (apparatus: Zenit-V, Kiev 16-U, SKS-1M, and Pentatset).

In order to measure the nonsteady component of the feed pressure, piezometric and inductive sensors with working frequencies of 2-10 kHz and with an output of the readings on the oscilloscope were used; for measuring the total and static pressures a Pitot microtube was used. The average pressure and flow rate of the gas were determined by means of damped sensors, manometers, and rotameters. The estimates of the measurement error carried out gave the following results: for pressure $\leq$ 3-5% and for gas flow rate $\leq$ 8-10%. The motion of the liquid in the tank was investigated by means of hydrokinematic indicators — particles with a specific gravity close to the specific gravity of the liquid. The trajectories of the particles were recorded with moving-picture and still-photographic equipment. In order to study conditions with a small quantity of gas in the liquid, a trace method was used [1]. For intense blowing conditions (the most interesting in practice), which were characterized by a reduction of transparency of the tank, the coordinates of individual particles with a diameter of $(2\text{-}10)\cdot10^{-3}$ m were recorded continuously [2].

For processing the moving-picture and still frames, a photoenlarger and an "LÉTI" slide projector were used. The characteristic interaction parameters were photographed from the flow fragments projected on the screen. For this, the visualization error was $\leq$ 5%, but in the case of visibility deterioration as a result of intense gas-saturation of the tank it was $\leq$ 10-15%.

The investigations were conducted over a wide range of sizes and shapes of the tank; geometries, sizes, and locations of the nozzles; physical properties of the gases and liquids; and blowing conditions (Fig. 1 and Table 1). In order to estimate the effect of density of the liquid on the length of the jet, experiments were carried out on an axisymmetrical model with pressure charging, which enabled the effect of the hydrostatic pressure of a column of liquid P_H and its density to be distinguished as a physical parameter (Fig. 1).

Analysis of the experimental data (length of jet in liquids l_1, l_2, and l_n, diameter d_1 and aperture angle Θ of the jet, and radius of curvature of the flotation trajectory of the jet R) was carried out by statistical methods (Fig. 2).

Institute of Mechanics, Leningrad. Translated from Inzhenerno-Fizicheskii Zhurnal, Vol. 33, No. 2, pp. 213-223, August, 1977. Original article submitted July 26, 1976.

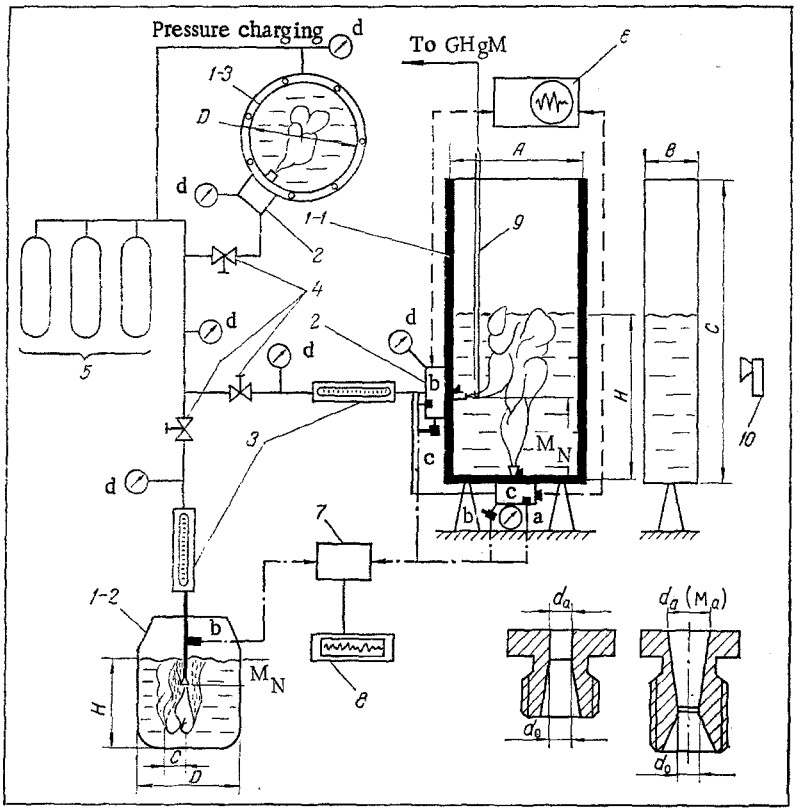

Fig. 1. Diagram of model complex: a) piezotransducer; b) DD-10 inductive sensor; c) DD-10 sensor with damper; d) manometer; 1 — 1) plane model; 1 — 2) model "converter"; 1 — 3) model "cylinder" with pressure charging; 2) receiver; 3) rotameters RS-3 to RS-7; 4) valve; 5) gas bottles; 6) cathode-ray oscilloscope ÉNO-1; 7) ID-2I amplifier; 8) K-701 loop oscillograph; 9) Pitot microtube; 10) moving-picture and still-photographic equipment.

The averaged values of the length of the jet in the liquid, found with a quite high confidence coefficient, were then used for obtaining the criterial relation $\bar{l} = l/d_0 = A(\rho/\rho_l)^{n_1} \cdot Fr^{n_2}We^{n_3}$ by linear regression methods [4], the choice of which will be justified below.

The statistical processing of the results of the experiment and of the regressing analysis were carried out on an M-222 computer.

Mechanism of Discharge of the Jet into the Liquid

In studying the mechanism of interaction, the majority of the investigations dwelt on the steady-state system. The results offered take account of the pulsation nature of discharge of the gas jets. Four gasdynamic discharge cycles of the jets are recognized (Fig. 2).

The bubble cycle is obtained in the case of excess pressures of the gas feed close to the hydrostatic pressure at the nozzle scarf $P_0 \leqslant (0.05\text{-}0.08)\cdot 10^5$ N/m^2 for an air discharge velocity of $V_a \leqslant$ 30-40 m/sec. At the nozzle scarf, gas bubbles are formed periodically; the size, shape, and frequency of breakaway are determined by the flow rate and the properties of the gas and liquid. The breakaway frequency of the bubbles varies from 5-10 Hz with increase of p_0 and is independent of the gas properties. When using viscous liquids, for example, glycerin, the size of the bubbles is increased, the spherical shape which is characteristic for water is distorted, and the breakaway frequency falls to 1 to 3 Hz. In the case of discharge from the upper immersed nozzle, in consequence of the countereffect of the gas stream pulse and Archimedean forces, the bubble is squashed and acquires the shape of an ellipsoid. For the bottom nozzles, the reverse pattern of elongation of the unseparated bubble is observed.

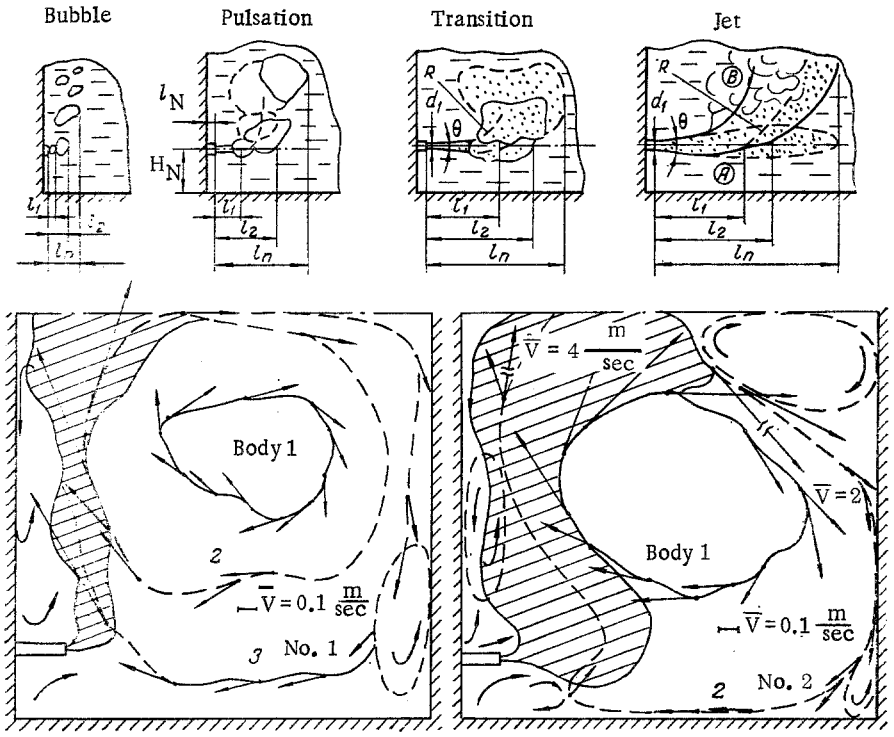

Fig. 2. Hydrogasdynamic models of the discharge of a jet and the circulation of the liquid with lateral gas feed. Air—water, plane tank. A = 0.494 m; B = 0.1 m; C = 1.2 m; H_N = 0.14 m; $d_\alpha = d_0 = 3 \cdot 10^{-3}$ m; H = 0.5 m; No. 1) $P_0 = 1.3 \cdot 10^5$ N/m²; No. 2) $P_0 = 3 \cdot 10^5$ N/m². Bodies 1-3 are hydrokinematic indicators.

The pulsed cycle [with excess pressure of $(0.08\text{-}0.1) \cdot 10^5 \leqslant P_0 \leqslant (0.3\text{-}0.5) \cdot 10^5$ N/m² for air discharge velocity V_α = 60-200 m/sec] is characterized by the formation and breakaway with a frequency of 10-15 Hz of coarser bubbles — ellipsoids — extended along the axis of the nozzle and by the formation at the nozzle scarf of a "foot" — a gas bridge in the form of a flexible shaft which is stable at the instant of breakaway of the gas mass and which is the embryo of a new bubble. The length of the "foot" increases with increase of P_0. The nature of the breakaway of the bubble for a lateral nozzle may be different. Separation of the gas mass from the horizontal "foot" with subsequent distortion of its shape and with fractionation during free floating is possible. However, another process is more probable: Under the action of the Archimedean forces, the gas mass, while maintaining its link with the "foot," floats upward and bends it sharply. At the instant of breakaway of the bubble, a new gas formation originates at the end of the bent "foot."

The discharge of gas from the upper nozzle is accompanied by a reduction of the length of the bubble, by emersion of the unseparated mass along the "foot," and by the possible formation of a "small chain," the links of which are individual bouyant gas masses, joined by bridges. The stream is characterized by both longitudinal (10-15 Hz) and transverse flow pulsations relative to the axis of the nozzle with a frequency of about 1 Hz, accompanied by intense vibrations of the liquid in the tank. The formation and breakaway of purely gas masses are characteristic for the cycles considered, and in the prenozzle space and in the vicinity of the nozzle scarf weak (a few percent of the average values) pressure pulsations with a frequency of about 10 Hz are recorded, which agrees well with the data from the oscillograms.

The transition cycle [$(0.3\text{-}0.5) \cdot 10^5 \leq P_0 \leq (1.2\text{-}1.3) \cdot 10^5$ N/m², in the case of discharge of air from the orifice with $V_\alpha \leq 160$ to a m/sec] is different in principle from the previous cycle by the onset of a jet two-phase flow, for which both the undisrupted flow region behind the nozzle scarf and the separating masses are a gas—liquid mixture with a variable concentration of the liquid phase. For lateral nozzles, two alternatives of development of the gas stream are possible. The first is the "blind shaft regime," mentioned in [5] and characterized by the development of a jet along the axis of the nozzle. In this case, three sections (Fig. 2) can be distinguished: 1) a stable axisymmetrical region with Θ = 18-24° and with a diameter (the boundary pulses with a frequency of ∿10-100 Hz) increasing by a

TABLE 1. Parameters of Experimental Equipment

Model	Dimensions, mm	No. of nozzles	Nozzle diameter, mm	M_a	M, mm	M_0, mm	$P_0 \cdot 10^{+5}$, N/m^2	l, mm	$G \cdot 10^{-4}$, kg/sec	Substance	Density, kg/m^3
Plane A × B × C	300×200×500 494×100×1200 800×500×1500	1; 4	2—10	1—3,3	200—600	0—200	1,0—10,0	0—200	0—400	Air Oxygen Nitrogen	1,29 1,43 1,25
"Converter"	D=300	1; 4	2—4	1	200—400	0—150	1,0—10,0	0—100	0—75	Helium Carbon dioxide gas	0,18 1,98
"Cylinder" with pressure charging	D=400	1; 4	2—5	1	200—350	0—250	1,0—5,0	0—50	0—100	Water Solutions of Na_2SO_3 Glycerin and solutions of its derivatives	1000 1000—1030 1050—1260

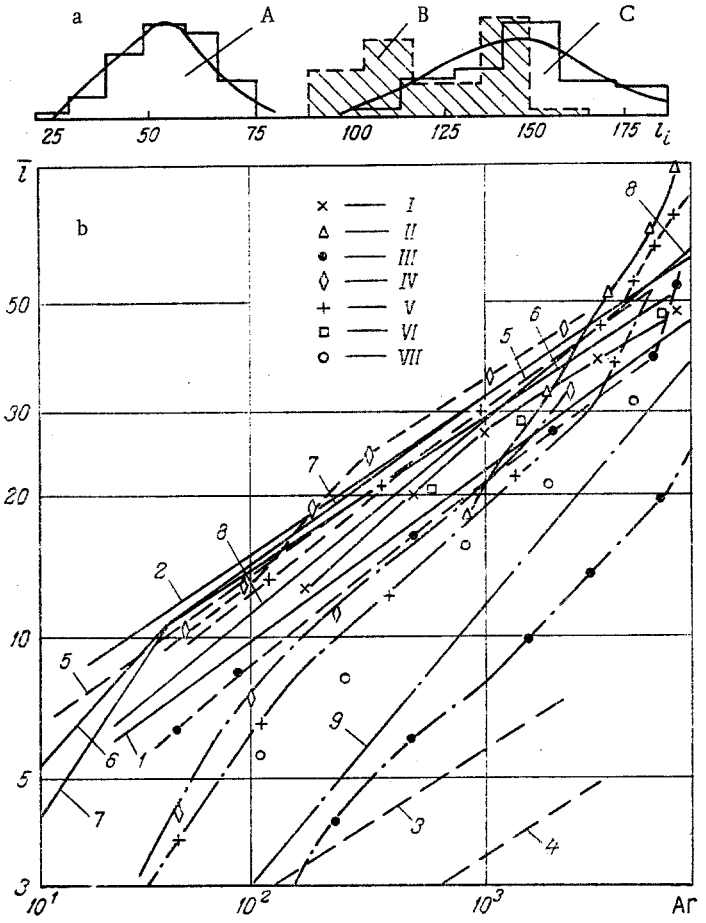

Fig. 3. Results of investigation of the depth of penetration of a gas jet into a liquid: a) histograms of the distribution of the instantaneous values of the "range" of a lateral jet: A) pulsation cycle, $P_0 = 0.3 \cdot 10^5$ N/m^2; B) transitional cycle, $P_0 = 1.3 \cdot 10^5$ N/m^2; C) jet cycle, $P_0 = 2.5 \cdot 10^5$ N/m^2; $d_0 = 3 \cdot 10^{-3}$ m, $M_a = 1$; air—water; x axis) $l_i \cdot 10^3$ m; y axis) number of measurements; b) dependence of dimensionless length of jet $\bar{l} = l/d_0$ on Ar: solid curves are vertical jets; dashed curves are maximum range l_2 of lateral jet; the dashed-dot curves are the minimum range (l_1) of the lateral jet; 1) [13]; 2) [6]; 3) [16] for $d_0 = 2 \cdot 10^{-3}$ m; 4) [16] for $d_0 = 10 \cdot 10^{-3}$ m; 5) [5]; 6) [5]; 7) [11]; 8, 9) calculation by formula (2). Experiment: I) $d_0 = 2 \cdot 10^{-3}$ m, $M_a = 1$, $H_N = 0$; II) $d_0 = 4 \cdot 10^{-3}$ m, $M_a = 1$, $H_N = 0.18$; III) $d_0 = 3 \cdot 10^{-3}$ m, $M_a = 1$, $H_N = 0.14$; IV) $d_0 = 3 \cdot 10^{-3}$ m, $M_a = 1$, water—air; V) $d_0 = 5 \cdot 10^{-3}$ m, $M_a = 1$; VI) $d_0 = 3 \cdot 10^{-3}$ m, $M_a = 1$, helium—glycerin; VII) value of l_i with a mathematical expectation of 0.99.

factor of 2 to 3 [$d_1 = (2\text{-}3)d_a$] due to the considerable "connected" mass of liquid in the vicinity of the nozzle scarf; 2) a "foot" of variable length and shape; 3) a pulsating mass, breaking away with a frequency of 10-15 Hz and then freely floating upward. The second alternative is characterized by a curvilinear trajectory with radius R, originating at the end of the axisymmetrical section due to the "foot," which is bent under the action of the buoyant gas (or more precisely, two-phase) mass, breakaway of which is possible on different sections of the trajectory. For upper nozzles, the first flow alternative is characteristic. In consequence of the lasting (less intensity in comparison with the pulsation cycle) vibrations of the liquid and the transverse instability of the jet, breakaway of the gas mass occurs during the maximum deviation of the jet from the axis of the vertical upper nozzle, attaining $C \approx 10d_0$ (Fig. 1).

The jet regime, in the case of excess pressure $P_0 \geq (1.2\text{-}1.5) \cdot 10^5$ N/m^2, is characterized by the formation of a two-phase jet with a turbulent boundary layer, pulsating over a

broad high-frequency spectrum. At lower pressures P_0, a flow which is close to the first considered variety of the transition regime with longitudinal stability — with breakaway of the masses with a frequency of 10-20 Hz — predominates. However, a stable jet development over the whole length is also possible. In this case, discharge of gas occurs by means of a bubbling of fine bubbles from the surface, with the exception of the initial axisymmetrical section. At large values of P_0, the turbulent two-phase jet, under the action of Archimedean forces, floats up along a curvilinear trajectory with radius of curvature R, which is significantly greater in comparison with the regimes considered previously. At the end of it [on the vertical section in the case of a large immersion of the nozzle (Fig. 1)], discharge of the gas takes place in the form of fine flushing bubbles or of large shapeless masses (for nozzles of large flow rate and diameter). However, under the action of random perturbations and at large values of P_0, individual "sheeting-through" of the jet along the axis of the nozzle, with the formation of a bubble inflowing at the nozzle, is possible.

In the case of flow from upper nozzles, a two-phase jet with a pulsating end from which coarse gas masses are separated with a frequency of $\sim$0.5 Hz is formed. The latter, on capturing the fine bubbles flushing from the surface, float along the edge of the jet, as a result of which the main jet moves as if in a gas "jacket," which increases its transverse stability and depth of penetration into the liquid. Experiments in tanks of different shapes and dimensions, with Laval nozzles having a Mach number at the scarf of $M_a = 1$ to 3.3, and with different capacities, a four-nozzle unit, and porous bodies have shown the identicalness of the gasdynamic regimes. The effect of the nature of the gas on the relative velocity (V_a/a), determining the regimes described, also was not observed.

The buoyant gas bubbles and the two-phase masses form a bubbling region, and a throw-out zone results at the surface during their discharge. In the case of small values of P_0, this region is localized in the vicinity of the nozzle wall for lateral nozzles. The motion of the liquid, initiated by the jet, promotes an even greater drift of bubbles in this direction (Fig. 2), which at considerable flow velocities (together with the pulsation of the jet) is the most important cause of the intensified destruction of the blast walls of metallurgical assemblies. With increase of P_0 and V_a, staggering of the nozzle l_N, and reduction of the initial level of liquid H, the throw-out zone may be transferred into the depth of the tank. The circulation motion of the liquid, of which the characteristics (trajectory and velocity vectors) for the plane tank in the case of the jet (No. 2) and pulsation (No. 1) regimes of lateral blowing are shown in Fig. 2, disperses the gas formation throughout the volume of the tank. As a result of this, below the edge of the lateral jet, just as in the region above the upper jets, the liquid contains almost no bubbles of gas. The shape and dimensions of the stable gas formations circulating in the tank are determined by the conditions of equilibrium and depend on the hydrostatic pressure in the layer of liquid and the nature of the gas and the liquid. Calculations according to the well-known relations [6, 7] have shown a satisfactory convergence with experiment; however, the actual spread of the dimensions (d = 2-6 mm for the sphere; d_{max} = 5-8 mm for the ellipsoid; and l_{max} = 6-15 mm for water) was wider.

An investigation of the gasdynamics of the tank revealed four regimes, characterized by different degrees of saturation of the liquid, with gas inclusions: bubble, jet, froth, and spray, partially considered in [5, 6, 8]. It should be noted that with a defined hydrodynamic regime which is characteristic for all the tanks, the formation of local regimes which differ from it is possible in individual regions. For example, with a total jet regime close to the surface of the bubble region, a froth and spray regime etc. are also possible (it is necessary to take this into account in practice). Despite the fact that the froth regime is the most effective from the point of view of mass transfer [9], and it originates by the intensification of blowing at the base of the jet, with a lateral gas feed the increase of P_0 and G plays a positive role only up to values which are defined for each nozzle. With increase of P_0 (Fig. 2), the jet may "block" the tank, separating it into a low-movement region below the jet with a low gas concentration A and an intensely circulating gas-saturated region above the jet B, in which the direction of motion is such that it promotes an accelerated ejection of gas from the tank. For all the immersed nozzles, independently of the shape and dimensions of the tank, with gas injection conditions specified for each nozzle diameter (H, P_0, G, V_a, H_N, and method of blowing), during the development of the jet in the liquid, large unstable gas masses are formed for which the flotation velocity and motion near the surface attain several meters per second, which exceeds by an order of magnitude the average velocity of the circulation flows throughout the volume of the tank [0.2 to 0.5 m/sec (Fig. 2)] and

which is greater than the velocity of the free flushing of bubbles [6, 7]. All this leads to an intense throw-out of gas from the tank, which, in consequence of the limited total interphase surface and small time of stay in the tank, is not able to enter into heat and mass exchange with the liquid and uselessly discharges into the atmosphere, sharply reducing the blowing efficiency — the so-called "breakdown" of the tank begins (the characteristics of this process are studied in [2, 3, 10]). This mechanism mainly also determines the laws of mass and heat transfer. The nature of the circulation and the velocity of motion of the liquid, depending on the shape and dimensions of the tank, play a secondary role, changing only the quantitative values of the parameters.

Depth of Penetration of the Jet into the Liquid

The depth of penetration of the jet into the liquid is the basic interaction parameter. For lateral jets, the depth of injection is characterized by the "range" l — the distance from the nozzle scarf to the intersection of the axis of the nozzle with the outside boundary of the gas stream — and the total length l_{tot} — the distance from the nozzle scarf to the outer boundaries of exit of the jet at the surface or to the vertical boundaries of the bubbling region (Fig. 1); for upper and inclined jets it is the distance along the axis from the nozzle scarf to the lower boundary of the jet (l). These characteristics have been studied by many authors [5, 6, 8, 11-16] (Fig. 3b); however, as can be seen from Fig. 3b, their data differ considerably, but mainly the various researchers expressed contradictory opinions concerning the effect of the physical properties of the gases and liquids, the diameter of the nozzle, and other parameters. For example, in [6], the effect of the density of the liquid is limited to 10%, but according to the data of [8] it changes l by a factor of 10.

Analysis of the histograms showed that in the case of longitudinal pulsations of the gas stream, the quantity l varied within the limits $l_1 - l_2$ (minimum and maximum "range," Fig. 2). In Fig. 3a, the distribution histograms for the instantaneous values of l_i of a lateral jet for three characteristic gasdynamic cycles are constructed. Analysis of the laws of the distribution, shown in the histogram, give a quantitative verification of the flow mechanisms presented earlier. Thus, for $P_0 = 1.3 \cdot 10^5$ N/m^2 [C], the values of l_i are grouped around two characteristic dimensions: $110 \cdot 10^{-3}$ m and $140 \cdot 10^{-3}$ m, corresponding to the two versions of jet development described above. For the cycle A, the most frequently achieved dimension lies midway between l_1 and l_2 and for C it is equal to $0.75 l_2$. The analysis carried out showed the validity of the assignment for the majority of cycles of a normal law of distribution (curves on cycles A and C of Fig. 3a). The most characteristic dimensions of the jet were determined for them (with a mathematical expectancy of 0.95 and 0.999). With a two-modal distribution (version B) the analysis is reduced to a division of the set of observations into two categories with its own law of distribution.

In Fig. 3b, in the form of the function $\bar{l} = l/d_0 = f(Ar)$, assumed by a number of researchers, the results of experiments are generalized for different conditions of lateral and top blowing over a range of Ar numbers; they exceed the well-known data by two orders of magnitude. Values obtained by other researchers over a considerably narrower range of values of Ar numbers and recalculated in this paper for convenience of their analysis and comparison with the cycles being studied are also given. It can be seen from the figure that the experimental values obtained for $\bar{l}_2$ coincide quite well with the data of the majority of researchers. The curves of $\bar{l}_1$ lie below, and the mismatch is increased with increase of the Ar number. The most characteristic jet lengths (with a mathematical expectancy of 0.99) occupy an intermediate position. Thus, for approximate calculations the use of any of the approximation relations is equally valid, but it is most convenient to determine the limiting values of l_1 and l_2 which define the region covered by the pulsating jet. The experimental curves shown in Fig. 3b adequately reflect the marked effect on the length of the jet of such parameters as the nozzle diameter, Mach number, and the physical properties of the gas and liquid. By using a complex of model tanks and media (Fig. 1, Table 1), a parametric investigation of the length l of a gas jet, in accordance with the following functional relation, was undertaken:

$$l = f(d_0,\ \alpha,\ n_N, H_N, V_a,\ M_a,\ P_0,\ \rho,\ \rho_l, \nu, \nu_l, \sigma_l,\ \text{method of blowing}).$$

The experimental curves of $\bar{l}$ ($\bar{l}_1$, $\bar{l}_2$) = f(P_0, I) are plotted for a lateral and an upper nozzle, where $I = \rho_a V_a (\pi/4) d_a^2 + (P_a - P_H)(\pi/4) d_a^2$. From comparison of the curves, the good agreement of the results can be seen for the lateral and upper jets, developing in the liquid according to a single law; however, in consequence of the reasons considered earlier, the upper jets are shorter than the lateral jets for small values of P_0, G, and I, but penetrate

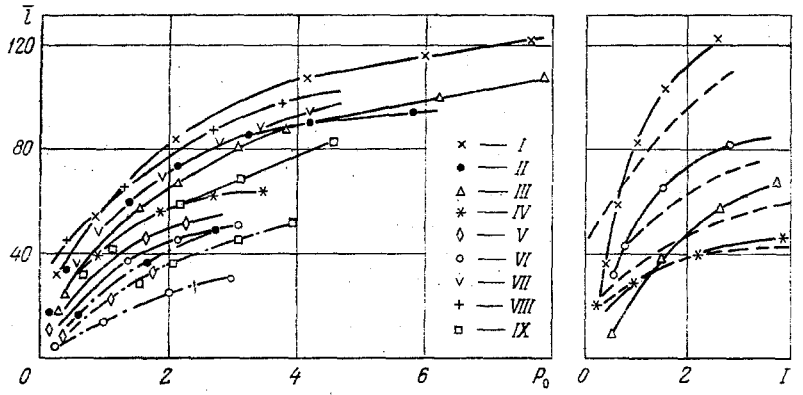

Fig. 4. Dependence of dimensionless length of an upper jet $\bar{l} = l/d_0 \cdot 10^3$ m and the dimensionless ranges $\bar{l}_1 = l_1/d_0$ and $\bar{l}_2 = l_2/d_0$ of a lateral jet on the excess feed pressure $P_0 \cdot 10^{-5}$ N/m^2 and the momentum of the jet I, kg/sec^2; solid curve is $\bar{l}$, $\bar{l}_2$; dashed-dot curve is $\bar{l}_1$; dashed curve is a calculation by formula (3). Experiment: I) $d_0 = 2 \cdot 10^{-3}$ m, H = 0.5; $H_N = 0$ — vertical jet; II) $d_0 = 3 \cdot 10^{-3}$ m, H = 0.5, $H_N = 0.14$ — lateral jet; III) $d_0 = 4 \cdot 10^{-3}$ m, $H_N = 0.18$ — vertical jet; IV-VII) lateral jet, water—air; IV) $d_0 = 5 \cdot 10^{-3}$ m, $M_a = 1$; V) $d_0 = 10 \cdot 10^{-3}$ m, $M_a = 1$; VI) $d_{01} = 3.5 \cdot 10^{-3}$ m, $n_N = 4$, $M_a = 2$; VII) $d_0 = 3 \cdot 10^{-3}$ m, $M_a = 1.6$; VIII) $d_0 = 3 \cdot 10^{-3}$ m, $M_a = 1$ — lateral jet, helium—water; IX) $d_0 = 5 \cdot 10^{-3}$ m, $M_a = 1.2$

deeper into the liquid with intense blowing. On all the graphs, stratification of the curves with respect to nozzle diameter amounting to 20-30% is marked, which confirms the results of [16] and contradicts the data of [5, 6]. A study of Laval nozzles showed, with similarity of the gasdynamic cycles, a negative effect of M_a on the depth of injection of the jet in the liquid, in consequence of the loss when achieving a detached flow in a diffusion nozzle. At the same time, in cycles close to the calculated cycle, $m = P_a/P_H = 1$, the range of the jet from a Laval nozzle becomes greater. Blowings with a four-nozzle assembly showed identicalness of the values of $\bar{l} = l/d_{01}$ with a single nozzle; i.e., the absolute depth of penetration of a unit-type jet in the tank is approximately less by a factor of two. A study of physical properties of the gases and liquids revealed a marked effect of such parameters as ρ, ρl, and σl, attaining 15-25%, and an independence of l from ν and νl. The effect of hydrostatic pressure on the nozzle scarf P_H was studied on a facility with forced blowing (Fig. 1). It was shown that with increase of P_H the length of the jet can be reduced by a factor of 10, since in this case the discharge velocity V_a of the gas falls sharply and, consequently, a change of the gasdynamic cycles determining it also begins. Thus, it is not the physical parameter ρl as was maintained in [8], but the weight of the corresponding column of liquid which determines the values of $l(\bar{l})$. The latter allows the results of the model experiments to be transferred unambiguously to the natural processes, which was confirmed by a comparison of the results with blowings in metal melts [8].

Taking account of the discovered independent effect of the principal determining parameters ρ, ρl, σl, d_0, P_0, P_a, and P_H, a refined approximation formula was obtained for the maximum and minimum lengths of the gas stream by regression analysis methods:

$$\bar{l}_2 = l_2/d_0 = 0.17\,(\mathrm{Fr})^{0.5}\,\bar{\rho}^{0.22}\,\mathrm{We}^{-0.32},$$
$$\bar{l}_1 = l_1/d_0 = 0.0045\,\mathrm{Fr}^{0.78}\,\bar{\rho}^{0.5}\,\mathrm{We}^{-0.67}, \qquad (1)$$

for which the error of the calculations does not exceed the experimental error, i.e., 10%. For approximate estimates, a formula which always describes the field of spread of the experimental values of l_1 and l_2 and which includes Ar numbers exceeding the well-known literature results ($50 \leq \mathrm{Ar} \leq 10^5$) by two orders of magnitude

$$\bar{l}_1 = 0.27\ \mathrm{Ar}^{0.56};\ \bar{l}_2 = 1.85\ \mathrm{Ar}^{0.4} \qquad (2)$$

was obtained with this method. The error of calculations by this formula is $\leq 20\%$. The latter approximation assumed in the literature, as can be seen from Fig. 3b, becomes inapplicable

when studying supercritical and supersonic conditions (regions of sharp breaks of the straight lines). In this case, the modified formula of Markov [6] can be recommended for approximate calculations:

$$\bar{l} \simeq \bar{l}_2 = 3{,}25 \sqrt[3]{\frac{I}{\rho_l g d_0^3}}. \qquad (3)$$

The agreement of calculations by this formula with experiment is shown in Fig. 4. The total length of the jet l_{tot} for different gasdynamic discharge cycles amounts to $(1.1\text{-}1.8)l_2$, and the radius of curvature R can be calculated according to [5, 3, 16]. The determination of the length of the jet for bottom nozzles is difficult because of the possibility of splitting of the main and bubbling streams.

NOTATION

P_0, ρ, ν, G, a, excess feed pressure, density, kinematic viscosity, gas flow rate per sec, and velocity of sound in the gas; V_a, M_a, P_a, ρ_a, discharge velocity, Mach number, static pressure, and density of the gas at the nozzle scarf; ρ_l, ν_l, σ_l, density, kinematic viscosity, and coefficient of surface tension of the liquid; d_0, d_a, diameter of the throat and outlet sections of the nozzle; n_N, number of nozzles; $Ar = \rho_a V_a^2/\rho_l g d_0$; $Fr = V_a^2/g d_0$; $We = \sigma_l/\rho_l g d_0$; $\bar{\rho} = \rho/\rho_l$; α, angle of inclination of nozzle.

LITERATURE CITED

1. V. S. Tolachev, I. V. Chepura, and V. P. Pavlov, Teor. Osn. Khim. Tekhnol., 6, No. 2 (1973).
2. I. P. Ginzburg, V. A. Surin, et al., in: Interuniversity Collection: Hydroaeromechanics and the Theory of Elasticity [in Russian], No. 22, Izd. DGU (1977), p. 3.
3. Report on Scientific-Research Work, Topic R13-3567, State Recording No. 74047532, Inventorial No. B541312, Leningrad Institute of Mechanics (1976).
4. N. Draper and H. Smith, Applied Regression Analysis, Wiley (1966).
5. A. V. Grechko, Author's Abstract of Candidate's Dissertation, MISiS (1972).
6. B. L. Markov, Methods of Purging an Open-Hearth Vat [in Russian], Metallurgiya, Moscow (1975).
7. V. I. Baptizmanskii et al., Izv. Vyssh. Uchebn. Zaved., Chern. Metallurg., No. 10 (1974).
8. A. V. Spesivtsev, Author's Abstract of Candidate's Dissertation, MISiS (1973).
9. I. P. Mukhlenov, M. E. Pozin, et al., Zh. Prikl. Khim., 27, No. 1 (1954).
10. Reports on Scientific-Research Work, Topic R13-3567, State Recording No. 74047532, Inventorial No. B338147 (1974); B436076 (1975), Leningrad Institute of Mechanics.
11. E. O. Khmelevskaya, Author's Abstract of Candidate's Dissertation MISiS—MÉI (1966).
12. I. G. Kazantsev, Stal', No. 1 (1940).
13. G. P. Ivantsov, in: Proceedings of the Scientific and Technical Society, Ferrous Metallurgy [in Russian], Vol. 18, Metallurgizdat (1957), p. 751.
14. V. I. Yavoiskii, G. A. Dorofeev, and I. L. Povkh, Theory of Purging a Steel Smelting Vat [in Russian], Metallurgiya, Moscow (1974).
15. B. L. Markov and L. A. Kirsanov, Izv. Vyssh. Uchebn. Zaved, Chern. Metallurg., No. 8 (1970).
16. I. A. Lebedinskaya, M. Z. Zhivov, B. S. Endler, et al., "Propagation of a horizontal gas jet in a heavy liquid," Tr. Inst. Gipronikel', No. 57, 86 (1973).